Chapter 6
Easily Accessible, Highly Potent, Photocontrolled Modulators of Bacterial Communication

External control of bacterial communication – quorum sensing – allows for the regulation of a multitude of biological processes. In this chapter, we describe the development of new synthetic methodology, as well as the characterization, photoisomerization and biological evaluation of a privileged series of novel photoswitchable quorum sensing agonists and antagonists. The presented method allows for the rapid and convenient synthesis of previously unknown photoswitchable agonists with up to 70% quorum sensing induction and inhibitors reaching up to 40% inhibition, which significantly extends the level of photocontrol over bacterial communication achieved before. Remarkably, for the lead photoswitchable agonist a >700 times difference in activity was observed between the irradiated and non-irradiated form, showing unprecedented levels of control in photopharmacology.

Manuscript submitted for publication as**: Easily Accessible, Highly Potent, Photocontrolled Modulators of Bacterial Communication.** M. J. Hansen, J. I. C. Hille, W. Szymanski, A. J. M. Driessen and B. L. Feringa. We greatly acknowledge J. I. C. Hille for his contribution to this chapter during his Master's thesis research.

6.1 Introduction

Bacterial communication plays a vital role in the regulation of symbiotic processes and pathogenesis of infections.[1–5] The communication between bacteria is mainly based on quorum sensing (QS); a process in which bacteria produce and excrete QS autoinducers that are responsible for upregulation of gene expression to control cellular organization, virulence and biofilm formation, amongst others.[3,5] External control over the activity of QS autoinducers would allow to up- or downregulate gene expression in bacteria, enabling remote regulation of for example biofilm formation, which is becoming a major threat in the treatment of bacterial infections, with serious implications in surgery.[6–9] Moreover, complementary to the field of optogenetics, genetic engineering combined with the external control of QS induction potentially allows to regulate a plethora of functions by controlling the activity of the QS operon with light.[10,11]

Light has proven to be an excellent stimulus for the remote control of biological systems.[12,13] In this context, the emerging field of photopharmacology aims at the design and synthesis of bioactive molecules, whose activity can be altered with light.[14–17] Photopharmacology relies on molecular photoswitches to control the structure of bioactive molecules in space and time. Incorporation of photoswitches into the pharmacophore renders the product reversibly photoresponsive. Applying the photopharmacological approach, a variety of biological targets and tools have been controlled ranging from ion channels,[18,19] glutamate receptors,[20,21] GPCRs,[22] to antibiotics,[23–25] and anti-tumor drugs.[26–28] In the context of quorum sensing, earlier work by our group focused on the design of photoswitchable QS autoinducers which lead to the photocontrol of QS-related gene expression and pyocyanin production.[29] This proof of concept, together with an abundance of synthetic QS ligands developed,[30–32] has paved the way for the further advancement toward more potent/selective autoinducers which can be controlled with light.

Two of the major native autoinducer motifs in *P. aeruginosa*, *N*-3-(oxododecanoyl)-L-homoserine lactone (OdDHL) and *N*-3-(oxododecanoyl)-L-homoserine lactone (BHL), are depicted in Figure 1.[33] These autoinducers both consist of a homoserine lactone 'head-group' and a hydrophobic alkyl chain. Interestingly, large differences in activity have been observed upon minor alterations of the structure, and the specificity of autoinduction is highly dependent on the bacterial strain, allowing for selective addressing of virulent strains over the beneficial ones.[8,30] For example, in *P. aeruginosa*, the 3-oxo motif seems to be inherent to the ability to induce quorum sensing, while the BHL also shows agonistic properties albeit less pronounced.

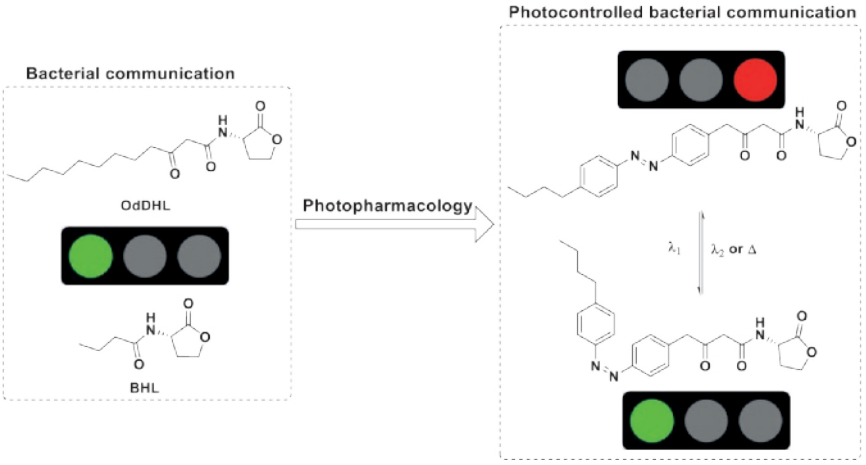

Figure 1. Concept of photocontrolled modulators of bacterial communication, starting from native QS autoinducers towards a photoswitchable agonist and antagonist toolbox.

6.2 Results and Discussion

Successful photomodulation of highly potent quorum sensing autoinducers requires the synthetic access to 3-oxo homoserine lactones. However, the photoswitchable derivatives of 3-oxo-homoserine lactone cannot be made via conventional synthetic methodology. While the original synthesis of the native 3-oxo derivative is performed using a low-yielding derivatization of Meldrum's acid that poses problems with both stability (decarboxylation) and purification when non-alkyl substrates are used,[34,35] efforts by the Blackwell group led to the development of an elegant, microwave-assisted synthetic sequence.[36] However, simple dianion formation, and nucleophilic substitution, in our hands, did not give satisfying results either; especially the reported protection/deprotection strategy proved troublesome with our azobenzene-based substrates, while we anticipated that elevated temperatures with microwave irradiation potentially poses problems with the photoswitch scaffold. In developing a new, efficient synthetic pathway towards aryl-substituted 3-oxo-homoserine lactones, we were inspired by earlier reports from the groups of Buchwald on the cross coupling of esters/ketones to aryl chlorides[37] and Skrydstrup on carbonylative vinylogous couplings with dioxinone,[38] which provided evidence that a novel, unprecedented cross coupling reaction between chlorobenzene and dioxinone could potentially allow the facile synthesis of a protected 3-oxo precursor. Our initial investigations focused on the development and optimization of such a cross coupling reaction to synthesize aryl-β-keto-amides.

A model reaction of chlorobenzene (1 eq) and dioxinone (1.1 eq) with catalytic ^{t}BuXPhos-Pd-G1 and 3 eq LiHMDS in toluene under ambient conditions for 30 min

yielded the desired coupling product **1** in remarkably high yield without the need for laborious purification (Figure 2c). To our delight, the reaction of *p*-chloroazobenzene (1 eq) with dioxinone (1 eq) under similar conditions also proceeded with >95% isolated yield after 30 min reaction time, without the need for chromatographic purification. Next, the synthesized intermediate was reacted with homoserine lactone in the presence of base at elevated temperatures (110 °C) to yield the desired photoswitchable 3-oxo-homoserine lactone **AHL1**. Full conversion was obtained after 3 h with only minor impurities, as observed from ^{1}H-NMR spectroscopy. Purification by flash chromatography yielded the pure product in satisfying yield. The versatility of this two-step method to prepare highly valuable aryl-3-oxo homoserine lactones was further demonstrated by the straightforward synthesis of a library of 16 photoresponsive effectors of bacterial communication (Figure 2d). A diverse set of both azobenzenes and different anilines or aminolactone could be used in a versatile two-step synthetic sequence from commercial available starting materials without the need for specific reaction optimization.

The library described here employs the azobenzene motif, an exceptional, versatile class of photoswitches with distinct photochemical properties.[39,40] The structure of azobenzene can be photochemically modulated between the thermally stable *trans*-isomer and the *cis*-isomer. The unstable *cis*-isomer converts thermally back to the *trans*-isomer over time or upon irradiation with another wavelength of light. Utilization of azobenzene derivatives, in a biological context, necessitates photochemical properties like high photostationary states, appropriate thermal half-lives and fatigue resistance, i.e. the ability to photoswitch for repetitive cycles without degradation. Photochemical and thermal isomerization studies were performed for all AHLs (see Figure 3 and Experimental section), exhibiting efficient photostationary states (>95% *trans* before irradiation, between 84% and 97% *cis* under irradiation, see Experimental section for details). Moreover, no significant fatigue was observed for any of the AHLs after five cycles of irradiation and half-lives for the *cis*-isomer showed to be between 28–100 min, which is within the suitable time range for the biological experiments performed (*vide infra*).

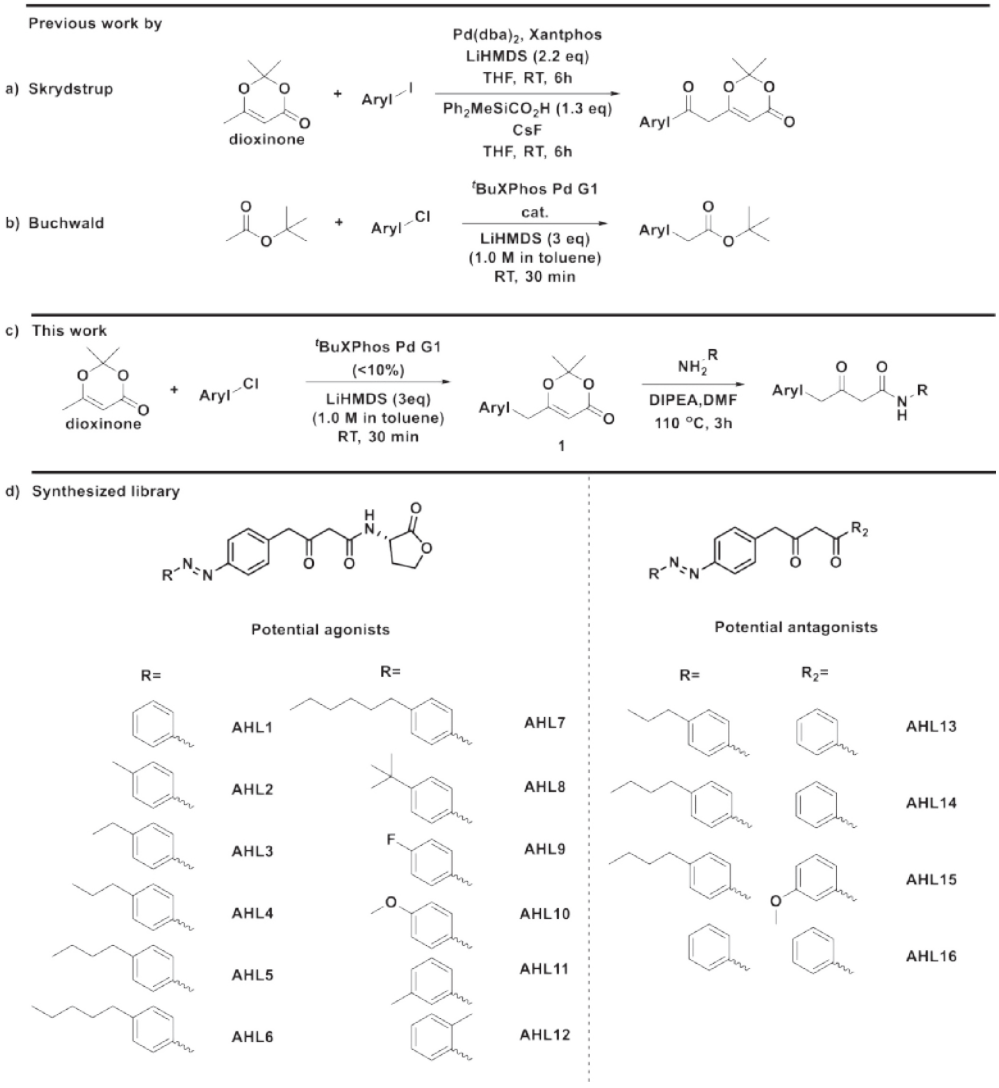

Figure 2. Synthetic methodology developed for the preparation of α- and β-carbonyl compounds. a,b) Previous work, reported cross couplings by Skrydstrup[38] and Buchwald.[37] c) This work; novel methodology for the synthesis of aryl-β-ketoamides. d) Synthesized library of potential agonists and antagonists. A diverse set of para-substituted AHLs has been prepared to investigate the structure-activity relationship.

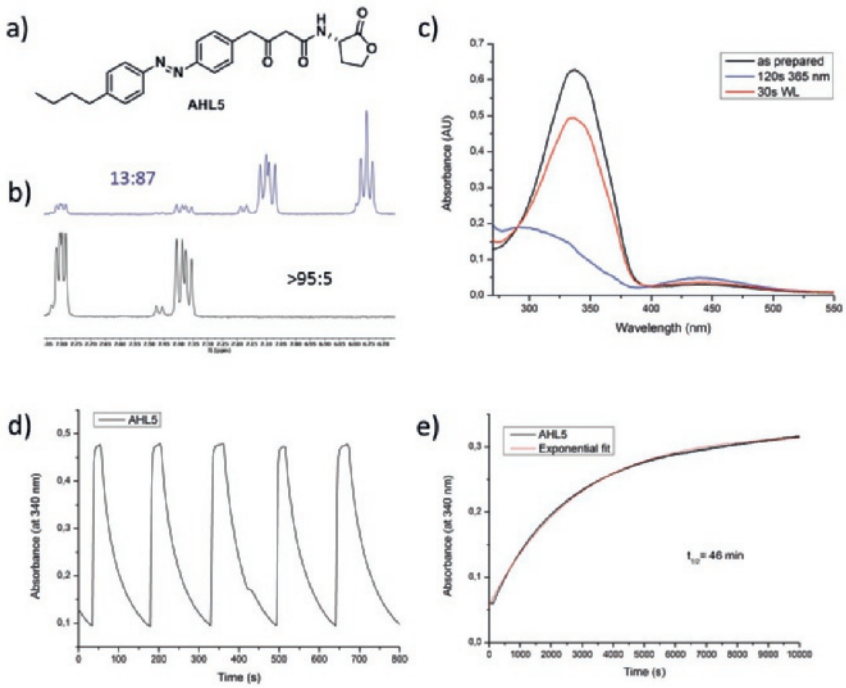

Figure 3. Photochemical evaluation of **AHL5**. a) Molecular structure of **AHL5**. b) Photostationary state and *trans-cis* ratio after thermal adaption of **AHL5**: thermally adapted (black) and 365nm irradiated (blue). c) UV-vis spectra showing the photoswitching of **AHL5** with an isosbestic point at 385 nm. d) Fatigue determination of **AHL5** with no significant fatigue observed after 5 rounds of irradiation. e) Kinetic evaluation of the half-life of **AHL5** at 30 °C. (All measurements are performed in DMSO at a concentration of 20 μM (or DMSO-d_6 at 2 mM for b)).

Subsequent biological evaluation focused on the Las network of *P. aeruginosa*, which can be quantified by the induction of LasQS as measured by a functional readout of bioluminescence in a QS reporter strain (*E.coli* JM109 pSB1075).[37] In this strain, the AHLs potentially bind to the transcriptional activator LasR to form a stable dimer, which can bind to the responsive promoter region of the LasQS system proceeding the *luxCDABE-lasR* promoter fusion reporter genes, resulting in enhanced bioluminescence. Initial studies focused on the potential quorum sensing inhibiting properties utilizing a competition experiment, in which the induction of the native OdDHL was inhibited with the different AHLs from the herein reported library (see Figure 6).[41,42] Compounds (**AHL13-15**) showed satisfactory inhibitory activity, as expected from earlier structure-activity-relationship (SAR) studies.[43,44] Also, **AHL1** showed good inhibitory activity against OdDHL with a minor difference in activity between the irradiated and non-irradiated samples. Inspired by these results, we synthesized and tested **AHL16**, which unfortunately exhibited similar inhibition with

a minor difference in activity. Notably, the 1-oxo-azo, reported before by our group,[29] proved to be the most potent photoswitchable inhibitor in our library with 57% inhibition of QS activity.

Next we tested the agonizing properties of the synthesized AHLs. Remarkably, only limited enhancement of the activity was observed for the 3-oxo **AHL1**, when compared to the previously reported 1-oxo-azo derivative,[29] whereas from previous structure activity relationship (SAR) studies[8,30] a considerable enhancement was expected. However, substitution of the azobenzene core had a major effect on the agonistic properties of the resulting photoswitchable AHLs. At the thermally stable states, both *p*-propyl and *p*-fluoro AHLs (**AHL4 and 9**) proved to be the main agonists of quorum sensing in this library with 15-18% induction (as compared to the native AHL, OdDHL, Figure 1). However, irradiation (λ = 365 nm for 5 min) of the AHLs and subsequent evaluation as quorum sensing agonists revealed a dramatic increase in activity for **AHLs 3-7** and **AHL10**, whereas the activity of **AHL9** showed a notable decrease (see Figure 4). Especially **AHL4** and **AHL5** stood out in this respect, with 71% and 46% QS induction, respectively. The activity of irradiated **AHL4** is closely comparable to the best known synthetic autoinducers reported so far.[8,31] From the small library reported herein, it can be concluded that the alkyl substituent at the *para*-position is crucial to enhance activity upon photoisomerization. As shown in Figure 4 (**AHL1-7**), elongation of the hydrophobic tail initially increases the activity reaching a maximum at the C_3 tail while further elongation up to a C_6 substituent leads to loss of activity.

Moreover, the selectivity of the *cis*-isomer (over the *trans*-isomer) also significantly changes with the substitution pattern. A profound 12-times difference in activity at a single concentration (5 μM) between the irradiated and non-irradiated form has been observed for **AHL5**. Subsequent investigation to the dose response of both the irradiated and non-irradiated **AHL5** (see Figure 5a) revealed a stunning >700-times difference in activity between the irradiated (*cis,* EC50 = 0.57μM) and non-irradiated (*trans,* no activity up to 400 μM, see Experimental section for details) forms. This difference in activity represents an unprecedented selectivity in photopharmacology, hitherto observed only for irreversible activation of photocaged systems,[45] and additionally illustrates the sensitivity of the LasQS system. Remarkably, the irradiated form shows a threshold at which activation reaches maximum. After 100 μM, the activity significantly decreases without interfering with bacterial growth (see Experimental section for growth curves). All the tested compounds showed no antibacterial activity, *i.e.* the AHLs did not alter the growth of the reporter strain at relevant concentrations (see Experimental section for growth curves), proving that the drop of the QS signal is not caused by compound toxicity and/or cell death.

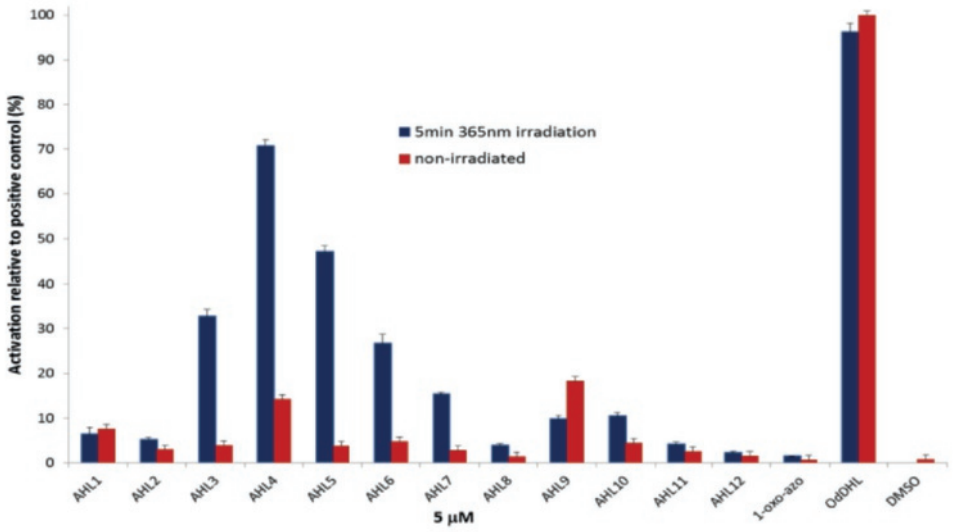

Figure 4. Biological evaluation of photocontrolled quorum sensing autoinducers. All compounds are evaluated at 5 µM with *E. coli* JM109 psB1075[42] as the reporter strain after 65 min of incubation. Native autoinducer OdDHL is used as positive control. Measurements are all mean of triplicates with standard deviation. AHLs are used in their thermally adapted form (red, *trans* isomer) or pre-irradiated (blue, mainly *cis* isomer) for 5 min with 365 nm light.

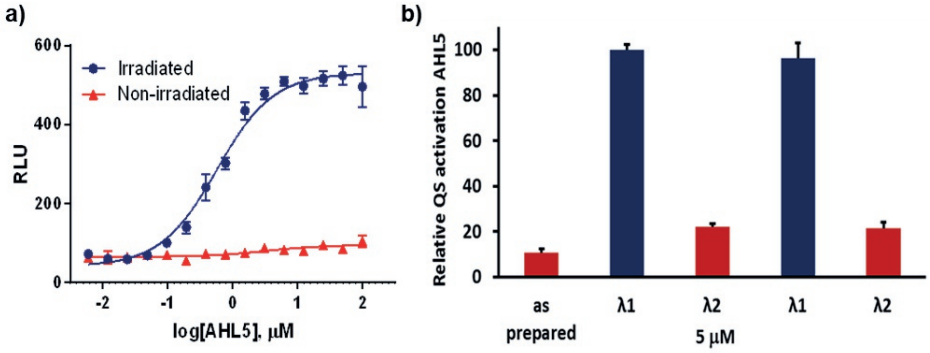

Figure 5. Dose-response profile and fatigue resistance of **AHL5**. a) Relative luminescence obtained at different concentrations of **AHL5**. A dramatic difference in agonizing activity is observed between irradiated and non-irradiated samples. b) Repetitive switching cycles without observable fatigue. λ1: 365nm for 5 min, λ2: white light for 1 min, 5 µM in LB with <1% DMSO.

To emphasize the reversibility of the induction attained with photoswitchable **AHL5**, and exclude the possibility that the difference in potency between the two forms of

AHL5 stems from photodegradation to a more potent compound, we sequentially activated and deactivated this compound with different wavelengths of light. As can be observed from Figure 5b, at least two cycles of activation-deactivation with 365 nm and WL are feasible without the observation of significant fatigue or degradation.

6.3 Conclusions

In conclusion, we have developed synthetic methodology to gain access to a library of photoswitchable 3-oxo derived QS agonists and antagonists via a novel Pd-catalyzed cross coupling reaction. Up to 71% QS induction was obtained, whereas the best synthesized inhibitor showed almost 40% OdDHL inhibition. Moreover, our lead compound, **AHL5**, showed privileged properties for further development in photopharmacology, due to an unprecedented difference in activity between the inactive (non-irradiated) and activated (irradiated) state. For the first time, utilizing reversible photoswitching, a more than 700-times difference in activity between the irradiated and non-irradiated forms has been achieved, allowing a complete on-off regulation of potency. Furthermore, the reversibility of photoswitchable **AHL5** has been attained without the observation of significant fatigue. Future studies in our laboratory will focus on the application of these AHLs to manipulate biofilm formation and toxin production in *P. aeruginosa*. The excellent on-off switching ability paves the way for future application of these novel photoswitchable QS agonists and distinct AHLs from the here reported series are highly promising as next-generation light-controlled research tools.

6.4 Experimental Section

6.4.1 General Remarks

For general remarks, see chapter 3.

6.4.2 Bacterial strains and growth conditions

E. coli JM109 containing the plasmid pSB1075 was grown in Luria Bertani (LB) broth, supplemented with 100 μg/ml ampicillin at 30 °C.

6.4.3 Bioluminescence assay

Overnight cultures (30 °C) of *E. coli* JM109 pSB1075 were diluted to OD= 0.02 in LB. Two dilution series of 100 μL LB with AHLs at the given concentration (final DMSO <1%) were prepared in a 96 wells plate. Half of the 96 well plate (white) was covered with an aluminum sticker to prevent light exposure. Subsequently, the plate was irradiated with λ = 365 nm for 5 min, after which 100 μL of the overnight cultures were added. To measure multiple rounds of switching between *cis*- and *trans*-isomers, plate was sequentially photo-irradiated at λ=365 nm for 5 min using a

Spectroline ENB-280C/FE UV lamp, followed by white light for 1 min using a Philips Plusline ES Small 160W 3100lm halogen lamp. This sequence was repeated twice. After every irradiation immediately, cell suspension was added to the designated wells and this part of the plate was covered with aluminum sticker to prevent light exposure.

After addition of both cell suspension and LB containing AHLs, the plates were incubated for 2-3 h at 30 °C in a white microtiter plate and the luminescence was measured every 5 min using a plate reader (Synergy H1, BioTek). The maximum luminescence, occurring after approximately 1 h, was used to compare the AHL caused induction of las activity. All measurements are at least triplicates providing mean values with standard deviation.

Inhibition was measured by a competition assay utilizing native QS autoinducer OdDHL (Sigma-Aldrich). OdDHL was dissolved at EC_{50} concentration (0.6 nM) in LB medium. This medium was used as a stock to prepare all samples. Subsequently, a dilution series of the different AHLs were dissolved at 80 μM concentration (<1% DMSO) in the stock LB. The series of AHLs was plated twice within the same plate and half of the plate was covered. Next, *E.coli* JM109 psB1075 was diluted to an OD = 0.02 in stock LB (with OdDHL). The uncovered part of the plate was irradiated with 365 nm for 5 min and subsequently the cover was removed and 100 mL cell suspension was added. Relative activity compared to a DMSO control was measured by bioluminescence output (Synergy H1, BioTek) and the relative inhibition was plotted (DMSO = 0% inhibition). All measurements are triplicates giving mean values with standard deviation.

6.4.4 Inhibition assay and growth curves

Growth curves at relevant concentrations were measured for all AHLs with and without irradiation for at least 10h. Assay conditions as described above were reproduced in a clear 96 wells plate to determine OD_{600} in a plate reader (Synergy H1, Biotek) at 30 °C. All measurements are triplicates. If required background correction was applied using OD_{600} (t=0) = 0.

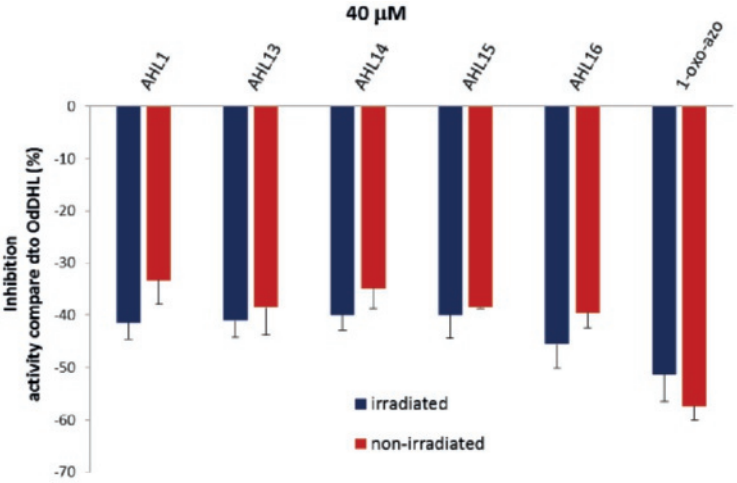

Figure 6. Inhibition of QS by photoswitchable AHLs (40 µM). QS measured by the bioluminescence output from *E. coli* JM109 pSB1075 reporter strain. Measurements are all mean values of triplicates with standard deviation. Zero-activity is induced by addition of 0.6 nM OdDHL (± EC_{50}) and relative decrease of activity is plotted as relative inhibition.

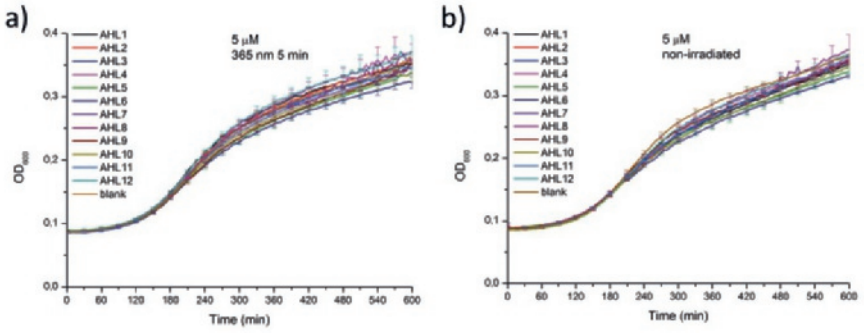

Figure 7. Growth curves for the *E. coli* reporter strain with the synthesized agonists (5 µM). Both the irradiated (a) and non-irradiated (b) forms were tested.

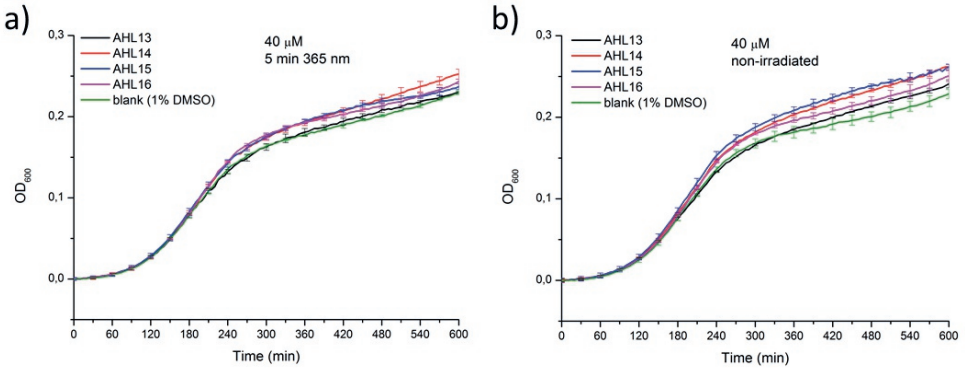

Figure 8. Growth curves for the *E. coli* reporter strain with the synthesized antagonists (40 μM). Both the irradiated (a) and non-irradiated (b) forms were tested.

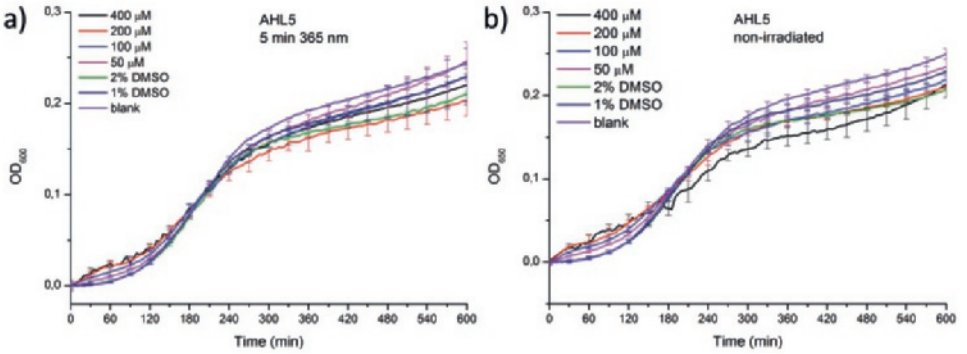

Figure 9. Growth curves for the *E. coli* reporter strain with **AHL5** at increasing concentrations. Both the irradiated (a) and non-irradiated (b) form were tested showing no significant difference in growth.

6.4.5 Synthesis

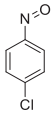

1-chloro-4-nitrosobenzene (**3**)

A mixture of 4-chloroaniline (3.00 g, 23.6 mmol), Oxone (14.4 g, 46.9 mmol), DCM (45 mL) and water (150 mL) was stirred at RT for 20 min until TLC indicated full conversion. Subsequently, the reaction mixture was extracted with DCM (3 x 50 mL), washed with aq. HCl (1M) solution (1 x 50 mL), sat. aq. $NaHCO_3$ (1 x 50 mL), brine (2

x 50 mL), dried with $MgSO_4$ and evaporated *in vacuo*. Flash chromatography (pentane) yielded the product as a yellow powder.

Crude yield: 34% (1.11 g), yellow powder

^{1}H NMR (400 MHz, DMSO-*d*$_6$): δ 7.97 (d, *J* = 8.6 Hz, 2H), 7.82 (d, *J* = 8.7 Hz, 2H).

Mills reaction

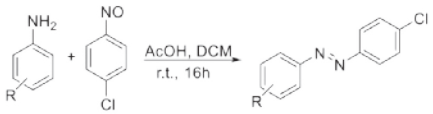

4-15

Compound **3** (1.40 mmol) and selected anilines (1.50 mmol) were dissolved in AcOH (7 mL) and DCM (7 mL) and stirred for 16 h at RT. Next, the mixture was poured into water (20 mL) and extracted with DCM (2 x 30 mL). The combined organic layers were washed with 1M aq. HCl (1 x 30 mL), sat. aq. $NaHCO_3$ (2 x 30 mL) and brine (30 mL) respectively, dried with $MgSO_4$ and evaporated *in vacuo* yielding the pure product (<5% *p*-chloro-nitrobenzene) after recrystallization from MeOH.

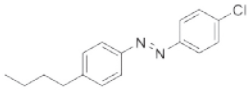

(E)-1-(4-butylphenyl)-2-(4-chlorophenyl)diazene **(9)**

Yield: 60% (230 mg), orange crystals

^{1}H NMR (400 MHz, $CDCl_3$): δ 7.84 (t, *J* = 8.0 Hz, 4H), 7.48 (d, *J* = 8.4 Hz, 2H), 7.32 (d, *J* = 8.1 Hz, 2H), 2.69 (t, *J* = 7.7 Hz, 2H), 1.70 – 1.60 (m, 2H), 1.45 – 1.33 (m, 2H), 0.95 (t, *J* = 7.3 Hz, 3H).

Pd-catalyzed cross coupling

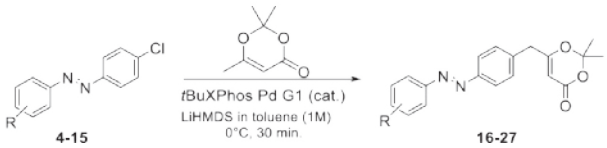

4-15 **16-27**

A dry Schlenk was equipped with stirring bar and septum and tBuXPhos Pd G1 (0.0043 mmol)was added under N_2-atmosphere at 0°C. Subsequently, *p*-chloro-azobenzene derivative (**4-15**) (0.43 mmol), 2,2,6-trimethyl-4H-1,3-dioxin-4-one (0.43 mmol) and LiHMDS (1M) in toluene (1.2 mmol) were added and the reaction mixture was stirred for 30 min at 0 °C. Next, the mixture was quenched with sat. aq. NH_4Cl (5 mL), extracted with EtOAc (3 x 20 mL), washed with brine (3 x 20 mL), dried with $MgSO_4$ and the volatiles were evaporated under reduced pressure resulting in the crude product.

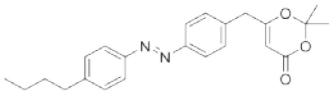

(E)-6-(4-((4-butylphenyl)diazenyl)benzyl)-2,2-dimethyl-4H-1,3-dioxin-4-one **(20)**

^{1}H NMR (400 MHz, $CDCl_3$): δ 7.90 – 7.81 (m, 4H), 7.34 (dd, *J* = 13.2, 8.1 Hz, 4H), 5.28 (s, 1H), 3.58 (s, 2H), 2.69 (t, *J* = 7.3 Hz, 2H), 1.66 (dd, *J* = 14.0, 6.0 Hz, 2H), 1.62 (s, 6H), 1.39 (dd, *J* = 14.1, 7.1 Hz, 2H), 0.94 (dd, *J* = 9.9, 4.5 Hz, 3H).

AHL formation

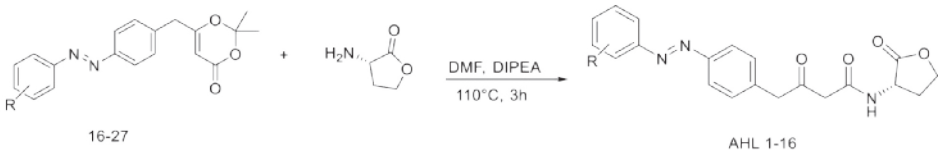

16-27 AHL 1-16

A mixture of crude (**16-27**) (0.43 mmol), (S)-(-)-α-Amino-γ-butyro lactone hydrobromide or aniline (0.43 mmol) and DIPEA (0.43 mmol) in DMF (1.2 mL) was stirred in a high pressure tube under N_2-atmosphere at 110 °C for 3 h. Subsequently, the mixture was dissolved in EtOAc (40 mL), extracted with brine (5 x 40 mL), dried ($MgSO_4$) and evaporated *in vacuo*. The crude product was purified by flash column chromatography (DCM: MeOH, 98:2) and subsequent precipitation in Et_2O yielded the pure photoswitchable AHLs.

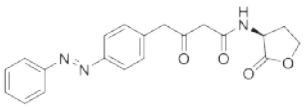

(E)-3-oxo-N-(2-oxotetrahydrofuran-3-yl)-4-(4-(phenyldiazenyl)phenyl)butanamide **(AHL1)**

Yield (over 2 steps): 52% (82 mg), yellow crystals

Melting point: 139-144°C

^{1}H NMR (400 MHz, DMSO-*d*$_6$): δ 8.65 (d, *J* = 7.8 Hz, 1H), 7.89 – 7.81 (m, 4H), 7.60 – 7.54 (m, *J* = 8.0 Hz, 3H), 7.38 (d, *J* = 8.3 Hz, 2H), 4.65 – 4.52 (m, 1H), 4.39 – 4.29 (m, *J* = 14.3, 7.2 Hz, 1H), 4.26 – 4.14 (m, 1H), 4.00 (s, 2H), 3.48 (s, 2H), 2.44 – 2.35 (m, 1H), 2.21 – 2.09 (m, *J* = 21.4, 10.8 Hz, 1H).

^{13}C NMR (100 MHz, DMSO-*d*$_6$): δ 202.1, 175.5, 166.6, 152.4, 151.2, 138.7, 131.9, 131.4, 129.9, 122.9, 122.9, 65.8, 50.5, 48.8, 48.6, 28.7.

HR-MS (ESI, [M+Na]$^+$): calculated for $C_{20}H_{19}N_3O_4$: 388.1268; Found: 388.1276

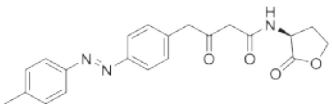

(R,E)-3-oxo-N-(2-oxotetrahydrofuran-3-yl)-4-(4-(p-tolyldiazenyl)phenyl)butanamide **(AHL2)**

Yield (over 2 steps): 37% (61 mg), orange crystals

Melting point: 185-187°C

^{1}H NMR (400 MHz, DMSO-*d*$_6$): δ 8.64 (d, *J* = 7.7 Hz, 1H), 7.84 – 7.75 (m, 4H), 7.38 (t, *J* = 8.4 Hz, 4H), 4.66 – 4.50 (m, 1H), 4.35 (t, *J* = 8.3 Hz, 1H), 4.20 (dd, *J* = 16.1, 9.5 Hz, 1H), 3.99 (s, 2H), 3.48 (s, 2H), 2.46 – 2.42 (m, 1H), 2.39 (s, 3H), 2.22 – 2.08 (m, 1H).

^{13}C NMR (100 MHz, DMSO-*d*$_6$): δ 202.2, 185.5, 166.6, 151.2, 150.5, 142.1, 138.3, 131.3, 130.4, 123.0, 122.8, 65.8, 50.5, 48.8, 48.6, 28.7, 21.5.

HR-MS (ESI, [M+Na]$^+$): calculated for $C_{21}H_{21}N_3O_4$: 402.1424; Found: 402.1432

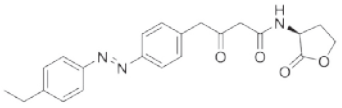

(R,E)-4-(4-((4-ethylphenyl)diazenyl)phenyl)-3-oxo-N-(2-oxotetrahydrofuran-3-yl)butanamide (**AHL3**)

Yield (over 2 steps): 38% (116 mg)

Melting point: 165-168 °C

^{1}H NMR (400 MHz, DMSO-*d*$_6$): δ 8.65 (d, *J* = 7.8 Hz, 1H), 7.81 (dd, *J* = 8.4, 3.5 Hz, 4H), 7.39 (dd, *J* = 16.6, 8.2 Hz, 4H), 4.62 – 4.54 (m, 1H), 4.40 – 4.32 (m, 1H), 4.21 (dddd, *J* = 9.7, 8.8, 6.4, 0.9 Hz, 1H), 3.99 (s, 2H), 3.48 (s, 2H), 2.69 (q, *J* = 7.6 Hz, 2H), 2.46 – 2.39 (m, 1H), 2.22 – 2.11 (m, 1H), 1.21 (td, *J* = 7.6, 0.9 Hz, 3H).

^{13}C NMR (100 MHz, DMSO-*d*$_6$): δ 202.1, 175.5, 166.6, 151.2, 150.7, 148.2, 138.3, 131.3, 129.2, 123.1, 122.7, 65.8, 50.4, 48.8, 48.6, 28.6, 28.5, 15.7.

HR-MS (ESI, [M+H]$^+$): calculated for $C_{22}H_{23}N_3O_4$: 393.17613; Found: 393.17453

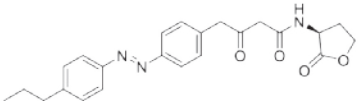

(R,E)-3-oxo-N-(2-oxotetrahydrofuran-3-yl)-4-(4-((4-propylphenyl)-diazenyl)-phenyl)butanamide (**AHL4**)

Yield (over 2 steps): 33% (55 mg)

Melting point: 150-154 °C

^{1}H NMR (400 MHz, DMSO-*d*$_6$): δ 8.65 (d, *J* = 7.8 Hz, 1H), 7.85 – 7.76 (m, 4H), 7.50 – 7.31 (m, 4H), 4.65 – 4.54 (m, 1H), 4.35 (td, *J* = 7.9, 7.1, 2.4 Hz, 1H), 4.23 – 4.17 (m, 1H),

3.99 (s, 2H), 3.48 (s, 2H), 2.63 (t, *J* = 7.6 Hz, 2H), 2.45 – 2.37 (m, 1H), 2.26 – 2.08 (m, 1H), 1.62 (q, *J* = 7.5 Hz, 2H), 0.90 (t, *J* = 7.3 Hz, 3H).

^{13}C NMR (100 MHz, DMSO-*d*$_6$): δ 202.1, 175.5, 166.6, 151.2, 150.7, 146.6, 138.3, 131.3, 129.8, 122.9, 122.78, 65.8, 50.4, 48.6, 37.4, 28.6, 24.3, 14.1.

HR-MS (ESI, [M+H]$^+$): calculated for $C_{23}H_{25}N_3O_4$: 407.19178; Found: 407.19008

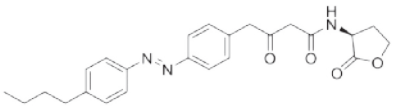

(R,E)-4-(4-((4-butylphenyl)diazenyl)phenyl)-3-oxo-N-(2-oxotetrahydrofuran-3-yl)butanamide **(AHL5)**

Yield (over 2 steps): 19% (34 mg), yellow crystals

Melting point: 158-162°C

^{1}H NMR (400 MHz, DMSO-*d*$_6$): δ 8.65 (d, *J* = 7.7 Hz, 1H), 7.81 (dd, *J* = 13.5, 6.6 Hz, 4H), 7.42 – 7.32 (m, 4H), 4.66 – 4.52 (m, *J* = 17.5, 9.4 Hz, 1H), 4.35 (t, *J* = 8.7 Hz, 1H), 4.20 (dd, *J* = 16.1, 9.4 Hz, 1H), 3.99 (s, 2H), 3.48 (s, 2H), 2.66 (t, *J* = 7.6 Hz, 2H), 2.44 – 2.36 (m, 1H), 2.24 – 2.04 (m, 1H), 1.64 – 1.52 (m, 2H), 1.38 – 1.25 (m, 2H), 0.89 (t, *J* = 7.3 Hz, 3H).

^{13}C NMR (100 MHz, DMSO-*d*$_6$): δ 202.2, 175.5, 166.6, 151.2, 150.7, 146.9, 138.3, 131.3, 129.7, 123.0, 122.8, 65.8, 50.5, 48.8, 48.6, 35.1, 33.3, 28.7, 22.2, 14.2.

HR-MS (ESI, [M+Na]$^+$): calculated for $C_{24}H_{27}N_3O_4$: 444.1894; Found: 444.1901

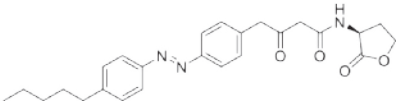

(R,E)-3-oxo-N-(2-oxotetrahydrofuran-3-yl)-4-(4-((4-pentylphenyl)-diazenyl)-phenyl)-butanamide (**AHL6**)

Yield (over 2 steps): 57% (119 mg)

Melting point: 156-159 °C

^{1}H NMR (400 MHz, DMSO-*d*$_6$): δ 8.65 (d, *J* = 7.8 Hz, 1H), 7.80 (dd, *J* = 8.4, 6.5 Hz, 4H), 7.38 (dd, *J* = 8.5, 7.0 Hz, 4H), 4.58 (ddd, *J* = 11.0, 9.1, 7.8 Hz, 1H), 4.35 (td, *J* = 8.8, 1.8 Hz, 1H), 4.21 (ddd, *J* = 10.6, 8.8, 6.4 Hz, 1H), 3.99 (s, 2H), 3.48 (s, 2H), 2.64 (t, *J* = 7.6 Hz, 2H), 2.44 – 2.39 (m, 1H), 2.16 (dtd, *J* = 12.1, 10.7, 8.9 Hz, 2H), 1.65 – 1.54 (m, 2H), 1.29 (tdd, *J* = 6.9, 4.0, 2.2 Hz, 4H), 0.85 (t, *J* = 6.8 Hz, 3H).

^{13}C NMR (100 MHz, DMSO-*d*$_6$): δ 202.1, 175.5, 166.6, 151.2, 150.6, 146.9, 138.3, 131.3, 129.7, 123.0, 122.7, 65.8, 50.4, 48.8, 48.6, 35.4, 31.3, 30.8, 28.6, 22.3, 14.3.

HR-MS (ESI, [M+H]$^+$): calculated for $C_{25}H_{29}N_3O_4$: 436.22308; Found: 436.22126

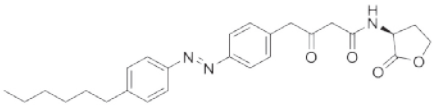

(R,E)-4-(4-((4-hexylphenyl)diazenyl)phenyl)-3-oxo-N-(2-oxotetrahydrofuran-3-yl)-butanamide **(AHL7)**

Yield (over 2 steps): 42% (81 mg), yellow crystals

Melting point: 156-164°C

^{1}H NMR (400 MHz, DMSO-*d*$_6$): δ 8.64 (d, *J* = 7.7 Hz, 1H), 7.80 (dd, *J* = 7.7, 6.0 Hz, 4H), 7.38 (dd, 4H), 4.67 – 4.51 (m, *J* = 17.4, 8.6 Hz, 1H), 4.39 – 4.28 (m, 1H), 4.25 – 4.14 (m, 1H), 3.98 (s, 2H), 3.48 (s, 2H), 2.65 (t, *J* = 7.6 Hz, 2H), 2.44 – 2.36 (m, *J* = 15.4, 5.1 Hz, 1H), 2.23 – 2.08 (m, 1H), 1.66 – 1.52 (m, *J* = 14.1, 6.8 Hz, 2H), 1.36 – 1.19 (m, *J* = 24.0 Hz, 6H), 0.84 (t, *J* = 6.6 Hz, 3H).

^{13}C NMR (100 MHz, DMSO-*d*$_6$): δ 202.2, 175.5, 166.6, 151.2, 150.7, 146.9, 138.3, 131.3, 129.7, 123.0, 122.8, 65.8, 50.5, 48.8, 48.6, 35.4, 31.5, 31.1, 28.7, 28.7, 22.5, 14.4.

HR-MS (ESI, [M+Na]$^+$): calculated for $C_{26}H_{31}N_3O_4$: 472.2207; Found: 472.2214

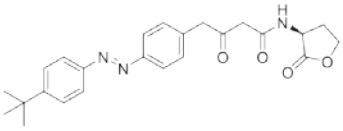

(R,E)-4-(4-((4-(tert-butyl)phenyl)diazenyl)phenyl)-3-oxo-N-(2-oxotetrahydrofuran-3-yl)butanamide **(AHL8)**

Yield (over 2 steps): 21% (38 mg), orange crystals

Melting point: 76-78°C

^{1}H NMR (400 MHz, DMSO-*d*$_6$): δ 8.65 (d, *J* = 7.7 Hz, 1H), 7.81 (d, *J* = 8.3 Hz, 4H), 7.60 (d, *J* = 8.5 Hz, 2H), 7.37 (d, *J* = 8.2 Hz, 2H), 4.63 – 4.53 (m, *J* = 17.3, 8.7 Hz, 1H), 4.38 – 4.30 (m, 1H), 4.25 – 4.16 (m, 1H), 3.99 (s, 2H), 3.48 (s, 2H), 2.44 – 2.37 (m, 1H), 2.20 – 2.09 (m, *J* = 21.1, 10.7 Hz, 1H), 1.32 (s, 9H).

^{13}C NMR (100 MHz, DMSO-*d*$_6$): δ 202.2, 175.5, 166.6, 154.9, 151.2, 150.4, 138.4, 131.3, 126.7, 122.8, 122.8, 65.8, 50.5, 48.8, 48.6, 35.2, 31.4, 28.7.

HR-MS (ESI, [M+Na]$^+$): calculated for $C_{24}H_{27}N_3O_4$: 444.1894; Found: 444.1899

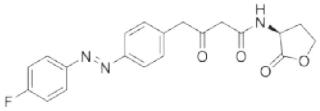

(R,E)-4-(4-((4-fluorophenyl)diazenyl)phenyl)-3-oxo-N-(2-oxotetrahydrofuran-3-yl)butanamide **(AHL9)**

Yield (over 2 steps): 26% (42 mg), orange/yellow crystals

Melting point: 158-162°C

^{1}H NMR (400 MHz, DMSO-*d*$_6$): δ 8.65 (d, *J* = 7.6 Hz, 1H), 7.95 (dd, *J* = 7.9, 5.5 Hz, 2H), 7.83 (d, *J* = 7.6 Hz, 2H), 7.45 – 7.33 (m, 4H), 4.57 (dd, *J* = 18.4, 9.1 Hz, 1H), 4.39 – 4.29 (m, 1H), 4.20 (dd, *J* = 15.9, 9.5 Hz, 1H), 3.99 (s, 2H), 3.48 (s, 2H), 2.45 – 2.36 (m, *J* = 8.6 Hz, 1H), 2.22 – 2.07 (m, *J* = 21.8, 10.9 Hz, 1H).

^{19}F NMR (376 MHz, DMSO-*d*$_6$): δ -109.25(m)

^{13}C NMR (100 MHz, DMSO-*d*$_6$): δ 202.1, 175.5, 166.6, 151.0, 149.1, 138.7, 131.4, 125.2, 122.9, 117.0, 116.8, 65.8, 50.5, 48.8, 48.6, 28.7.

HR-MS (ESI, [M+Na]$^+$): calculated for $C_{20}H_{18}FN_3O_4$: 406.1174; Found: 406.1179

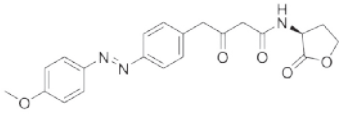

(R,E)-4-(4-((4-methoxyphenyl)diazenyl)phenyl)-3-oxo-N-(2-oxotetrahydrofuran-3-yl)butanamide **(AHL10)**

Yield (over 2 steps): 17% (28 mg), yellow crystals

Melting point: 163-168°C

^{1}H NMR (400 MHz, DMSO-*d*$_6$): δ 8.64 (d, *J* = 7.7 Hz, 1H), 7.87 (d, *J* = 8.8 Hz, 2H), 7.78 (d, *J* = 8.0 Hz, 2H), 7.35 (d, *J* = 8.1 Hz, 2H), 7.12 (d, *J* = 8.8 Hz, 2H), 4.64 – 4.52 (m, 1H), 4.35 (t, *J* = 8.6 Hz, 1H), 4.25 – 4.16 (m, 1H), 3.97 (s, 2H), 3.85 (s, 3H), 3.48 (s, 2H), 2.45 – 2.36 (m, *J* = 15.5, 5.3 Hz, 1H), 2.22 – 2.08 (m, *J* = 21.8, 10.8 Hz, 1H).

^{13}C NMR (100 MHz, DMSO-*d*$_6$): δ 220.2, 175.5, 166.6, 162.4, 151.3, 146.6, 137.8, 131.3, 125.0, 122.6, 115.1, 65.8, 56.1, 50.4, 48.8, 48.6, 28.7.

HR-MS (ESI, [M+Na]$^+$): calculated for $C_{21}H_{21}N_3O_5$: 418.1373; Found: 418.1382

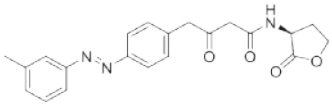

(R,E)-3-oxo-N-(2-oxotetrahydrofuran-3-yl)-4-(4-(m-tolyldiazenyl)-phenyl)-butanamide**(AHL11)**

Yield (over 2 steps): 37% (60 mg), orange/yellow crystals

Melting point: 132-137°C

^{1}H NMR (400 MHz, DMSO-*d*$_6$): δ 8.65 (d, *J* = 7.7 Hz, 1H), 7.87 – 7.80 (m, 2H), 7.68 (d, *J* = 6.3 Hz, 2H), 7.46 (t, *J* = 8.1 Hz, 1H), 7.42 – 7.33 (m, *J* = 8.1 Hz, 3H), 4.65 – 4.53 (m, *J* = 17.2, 7.6 Hz, 1H), 4.39 – 4.30 (m, *J* = 14.6, 7.4 Hz, 1H), 4.25 – 4.15 (m, 1H), 3.99

(s, 2H), 3.49 (s, 2H), 2.47 – 2.45 (m, 1H), 2.41 (s, 3H), 2.22 – 2.09 (m, *J* = 21.5, 10.8 Hz, 1H).

^{13}C NMR (100 MHz, DMSO-*d*$_6$): δ 202.2, 175.5, 166.6, 152.5, 151.2, 139.4, 138.6, 132.5, 131.4, 129.7, 122.9, 122.8, 120.6, 65.8, 50.5, 48.8, 48.6, 28.7, 21.3.

HR-MS (ESI, [M+Na]$^+$): calculated for $C_{21}H_{21}N_3O_4$: 402.1424; Found: 402.1433

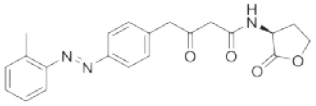

(R,E)-3-oxo-N-(2-oxotetrahydrofuran-3-yl)-4-(4-(o-tolyldiazenyl)-phenyl)-butanamide **(AHL12)**

Yield (over 2 steps): 29% (48 mg), orange/red crystals

Melting point: 107-111°C

^{1}H NMR (400 MHz, DMSO-*d*$_6$): δ 8.65 (d, *J* = 7.7 Hz, 1H), 7.83 (d, *J* = 8.2 Hz, 2H), 7.54 (d, *J* = 7.9 Hz, 1H), 7.42 (d, *J* = 3.0 Hz, 2H), 7.37 (d, *J* = 8.3 Hz, 2H), 7.33 – 7.27 (m, 1H), 4.64 – 4.53 (m, *J* = 19.0, 8.4 Hz, 1H), 4.38 – 4.31 (m, *J* = 8.9, 7.7 Hz, 1H), 4.24 – 4.17 (m, 1H), 3.99 (s, 2H), 3.48 (s, 2H), 2.65 (s, 3H), 2.44 – 2.37 (m, 1H), 2.21 – 2.09 (m, 1H).

^{13}C NMR (100 MHz, DMSO-*d*$_6$): δ 202.2, 175.5, 166.6, 151.6, 150.4, 138.4, 138.0, 131.9, 131.8, 131.3, 127.1, 123.0, 115.5, 65.8, 50.5, 48.8, 48.6, 28.7, 17.5.

HR-MS (ESI, [M+Na]$^+$): calculated for $C_{21}H_{21}N_3O_4$: 402.1424; Found: 402.1435

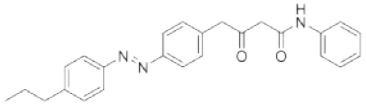

(*E*)-3-oxo-N-phenyl-4-(4-((4-propylphenyl)diazenyl)phenyl)butanamide (**AHL13**)

Yield (over 2 steps): 63% (138 mg)

Melting point: 117-121 °C

^{1}H NMR (400 MHz, DMSO-*d*$_6$): δ 7.88 (dd, *J* = 8.7, 1.7 Hz, 2H), 7.81 (dd, *J* = 8.4, 1.7 Hz, 2H), 7.64 (dd, *J* = 8.7, 1.7 Hz, 2H), 7.41 (dd, *J* = 8.4, 1.7 Hz, 2H), 5.74 (s, 1H), 2.64 (t, *J* = 8.3 Hz, 2H), 1.63 (q, *J* = 8.5, 8.0 Hz, 2H), 0.90 (t, *J* = 8.1 Hz, 3H).

^{13}C NMR (100 MHz, DMSO-*d*$_6$): δ 202.5, 165.3, 151.2, 150.7, 146.6, 139.3, 138.3, 131.3, 129.8, 129.2, 123.9, 122.9, 122.8, 119.5, 51.7, 49.1, 37.4, 24.3, 14.0.

HR-MS (ESI, [M+H]$^+$): calculated for $C_{25}H_{25}N_3O_2$: 400.20195; Found: 400.20045

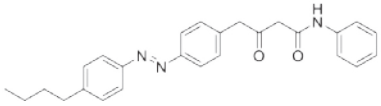

(*E*)-4-(4-((4-butylphenyl)diazenyl)phenyl)-3-oxo-N-phenylbutanamide (**AHL14**)

Yield (over 2 steps): 49% (84 mg)

Melting point: 149-151 °C

^{1}H NMR (400 MHz, DMSO-*d*$_6$): δ 10.09 (s, 1H), 7.86 – 7.76 (m, 4H), 7.56 (dd, *J* = 8.6, 1.2 Hz, 2H), 7.40 (dd, *J* = 8.5, 1.8 Hz, 4H), 7.29 (dd, *J* = 8.6, 7.4 Hz, 2H), 7.04 (t, *J* = 7.4 Hz, 1H), 4.03 (s, 2H), 3.66 (s, 2H), 2.66 (t, *J* = 7.7 Hz, 2H), 1.63 – 1.53 (m, 2H), 1.32 (h, *J* = 7.4 Hz, 2H), 0.90 (t, *J* = 7.4 Hz, 3H).

^{13}C NMR (100 MHz, DMSO-*d*$_6$): δ 202.5, 165.3, 151.2, 150.6, 146.8, 139.3, 138.3, 131.3, 129.7, 129.2, 123.9, 123.0, 122.8, 119.5, 51.78, 49.1, 35.1, 33.3, 22.2, 14.2.

HR-MS (ESI, [M+H]$^+$): calculated for $C_{26}H_{27}N_3O_2$: 414.21760; Found: 414.21618

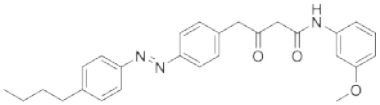

(*E*)-4-(4-((4-butylphenyl)diazenyl)phenyl)-N-(3-methoxyphenyl)-3-oxobutanamide (**AHL15**)

Yield (over 2 steps): 25% (48 mg)

Melting point: 114-117 °C

^{1}H NMR (400 MHz, DMSO-*d*$_6$): δ 10.07 (s, 1H), 7.83 – 7.78 (m, 4H), 7.42 – 7.38 (m, 4H), 7.25 (t, *J* = 2.2 Hz, 1H), 7.19 (t, *J* = 8.1 Hz, 1H), 7.11 – 7.06 (m, 1H), 6.63 (ddd, *J* = 8.2, 2.6, 0.9 Hz, 1H), 4.03 (s, 2H), 3.71 (s, 3H), 3.65 (s, 2H), 2.66 (t, *J* = 7.6 Hz, 2H), 1.65 – 1.53 (m, 2H), 1.32 (h, *J* = 7.4 Hz, 2H), 0.90 (t, *J* = 7.3 Hz, 3H).

^{13}C NMR (100 MHz, DMSO-*d*$_6$): δ 202.4, 165.3, 159.9, 151.2, 150.6, 146.8, 140.4, 138.2, 131.3, 130.0, 129.7, 123.0, 122.8, 111.8, 109.3, 105.3, 55.4, 51.8, 49.1, 35.1, 33.3, 22.2, 14.2.

HR-MS (ESI, [M+H]$^+$): calculated for $C_{27}H_{29}N_3O_3$: 444.22817; Found: 444.22655

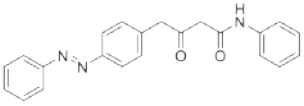

(*E*)-3-oxo-N-phenyl-4-(4-(phenyldiazenyl)phenyl)butanamide (**AHL16**)

Yield (over 2 steps): 35% (78 mg)

Melting point: 126-128 °C

^{1}H NMR (400 MHz, DMSO-*d*$_6$): δ 10.09 (s, 1H), 7.89 – 7.83 (m, 4H), 7.59 – 7.54 (m, 4H), 7.42 (d, *J* = 8.4 Hz, 2H), 7.29 (dd, *J* = 8.5, 7.4 Hz, 2H), 7.07 – 7.02 (m, 1H), 4.04 (s, 2H), 3.67 (s, 2H).

^{13}C NMR (100 MHz, DMSO-d_6): δ 202.5, 165.3, 152.4, 151.2, 139.3, 138.6, 131.8, 131.4, 129.9, 129.2, 123.9, 123.1, 122.9, 119.5, 51.8, 49.1.

HR-MS (ESI, [M+H]$^+$): calculated for $C_{22}H_{19}N_3O_2$: 358.15500; Found: 358.15385

6.4.6 Photochemical characterization

Table 1. *Trans:cis* ratios of the photoswitchable AHLs in DMSO-d_6, as determined by ^{1}H-NMR before and after irradiation with 365 nm (1h), at a concentration of 2 mM.

Compound	Non-irradiated (*trans:cis*)	PSS 365 nm (*trans:cis*)
AHL1	>95:5	11:89
AHL2	>95:5	9:91
AHL3	>95:5	8:92
AHL4	>95:5	6:94
AHL5	>95:5	13:87
AHL6	>95:5	7:93
AHL7	>95:5	10:90
AHL8	>95:5	5:95
AHL9	>95:5	15:85
AHL10	>95:5	16:84
AHL11	>95:5	16:84
AHL12	>95:5	10:90
AHL13	>95:5	3:97
AHL14	>95:5	7:93
AHL15	>95:5	8:92
AHL16	>95:5	11:89

6.5 References

(1) Greenberg, E. P. *Nature* **2003**, *424* 134–134.

(2) Camilli, A.; Bassler, B. L. *Science* **2006**, *311*, 1113–1116.

(3) Rasko, D. A.; Sperandio, V. *Nat. Rev. Drug Discov.* **2010**, *9*, 117–128.

(4) Fuqua, C.; Greenberg, E. P. *Nat. Rev. Mol. Cell Biol.* **2002**, *3*, 685–695.

(5) Welsh, M. A.; Blackwell, H. E. *FEMS Microbiol. Rev.* **2016**, *40*, 774–794.

(6) Stevens, A. M.; Queneau, Y.; Soulère, L.; Bodman, S. von; Doutheau, A. *Chem. Rev.* **2011**, *111*, 4–27.

(7) Fuqua, C.; Parsek, M. R.; Greenberg, E. P. *Annu. Rev. Genet.* **2001**, *35*, 439–468.

(8) Moore, J. D.; Rossi, F. M.; Welsh, M. A.; Nyffeler, K. E.; Blackwell, H. E. *J. Am. Chem. Soc.* **2015**, *137*, 14626–14639.

(9) Wysoczynski-Horita, C. L.; Boursier, M. E.; Hill, R.; Hansen, K.; Blackwell, H. E.; Churchill, M. E. A. *Molecular Microbiology* , **2018**, *108,* 240–257

(10) Young, D. D.; Deiters, A. *Angew. Chem.,Int. Ed.* **2007**, *46*, 4290–4292.

(11) Kramer, R. H.; Mourot, A.; Adesnik, H. *Nat. Neurosci.* **2013**, *16*, 816–823.

(12) Szymański, W.; Beierle, J. M.; Kistemaker, H. A. V.; Velema, W. A.; Feringa, B. L. *Chem. Rev.* **2013**, *113*, 6114–6178.

(13) Ankenbruck, N.; Courtney, T.; Naro, Y.; Deiters, A. *Angew. Chem., Int. Ed.* **2018**, 57, 2768–2798.

(14) Velema, W. A.; Szymanski, W.; Feringa, B. L. *J. Am. Chem. Soc.* **2014**, *136*, 2178–2191.

(15) Broichhagen, J.; Frank, J. A.; Trauner, D. *Acc. Chem. Res.* **2015**, *48*, 1947–1960.

(16) Lerch, M. M.; Hansen, M. J.; van Dam, G. M.; Szymanski, W.; Feringa, B. L. *Angew. Chem., Int. Ed.* **2016**, 55, 10978–10999.

(17) Hüll, K.; Morstein, J.; Trauner, D. *Chem. Rev.* **2018**, acs.chemrev.8b00037.

(18) Zemelman, B. V; Nesnas, N.; Lee, G. A.; Miesenbock, G. *Proc. Natl. Acad. Sci. U. S. A.* **2003**, *100*, 1352–1357.

(19) Kocer, A.; Walko, M.; Meijberg, W.; Feringa, B. L. *Science* **2005**, *309*, 755–758.

(20) Volgraf, M.; Gorostiza, P.; Numano, R.; Kramer, R. H.; Isacoff, E. Y.; Trauner, D. *Nat. Chem. Biol.* **2006**, *2*, 47–52.

(21) Reiner, A.; Isacoff, E. Y. *Nat. Chem. Biol.* **2014**, *10*, 273–280.

(22) Gómez-Santacana, X.; de Munnik, S. M.; Vijayachandran, P.; Da Costa Pereira, D.; Bebelman, J. P. M.; de Esch, I. J. P.; Vischer, H. F.; Wijtmans, M.; Leurs, R. A*ngew.Chem., Int. Ed.* **2018**, *57,* 11608 –11612

(23) Velema, W. A.; van der Berg, J. P.; Hansen, M. J.; Szymanski, W.; Driessen, A. J. M.; Feringa, B. L. *Nat. Chem.* **2013**, 5 , 924–928.

(24) Wegener, M.; Hansen, M. J.; Driessen, A. J. M.; Szymanski, W.; Feringa, B. L. *J. Am. Chem. Soc.* **2017**, *139*, 17979–17986.

(25) Weston, C. E.; Krämer, A.; Colin, F.; Yildiz, Ö.; Baud, M. G. J.; Meyer-Almes, F.-J.; Fuchter, M. J. *ACS Infect. Dis.* **2017**, *3*, 152–161.

(26) Hansen, M. J.; Velema, W. A.; de Bruin, G.; Overkleeft, H. S.; Szymanski, W.; Feringa, B. L. *ChemBioChem* **2014**, *15*, 2053–2057.

(27) Ferreira, R.; Nilsson, J. R.; Solano, C.; Andréasson, J.; Grøtli, M. *Sci. Rep.* **2015**, *5*, 9769.

(28) Simeth, N. A.; Altmann, L.-M.; Wössner, N.; Bauer, E.; Jung, M.; König, B. *J. Org. Chem.*, **2018**, *83*, 7919–7927

(29) Van der Berg, J. P.; Velema, W. A.; Szymanski, W.; Driessen, A. J. M.; Feringa, B. L. *Chem. Sci.* **2015**, *6*, 3593–3598.

(30) Geske, G. D.; O'Neill, J. C.; Miller, D. M.; Wezeman, R. J.; Mattmann, M. E.; Lin, Q.; Blackwell, H. E. *ChemBioChem* **2008**, *9*, 389–400.

(31) Boursier, M. E.; Manson, D. E.; Combs, J. B.; Blackwell, H. E. *Bioorg. Med. Chem.* **2018**, DOI:10.1016/j.bmc.2018.05.018

(32) Hodgkinson, J. T.; Galloway, W. R. J. D.; Wright, M.; Mati, I. K.; Nicholson, R. L.; Welch, M.; Spring, D. R. *Org. Biomol. Chem.* **2012**, *10*, 6032.

(33) Gerdt, J. P.; Wittenwyler, D. M.; Combs, J. B.; Boursier, M. E.; Brummond, J. W.; Xu, H.; Blackwell, H. E. *ACS Chem. Biol.* **2017**, *12*, 2457–2464.

(34) McInnis, C. E.; Blackwell, H. E. *Bioorg. Med. Chem.* **2011**, *19*, 4812–4819.

(35) Miller, L. C.; O'Loughlin, C. T.; Zhang, Z.; Siryaporn, A.; Silpe, J. E.; Bassler, B. L.; Semmelhack, M. F. *J. Med. Chem.* **2015**, *58*, 1298–1306.

(36) Geske, G. D.; Wezeman, R. J.; Siegel, A. P.; Blackwell, H. E. *J. Am. Chem. Soc.*, **2005**, *127*, 12762–12763

(37) Biscoe, M. R.; Buchwald, S. L. *Org. Lett.* **2009**, *11*, 1773–1775.

(38) Makarov, I. S.; Kuwahara, T.; Jusseau, X.; Ryu, I.; Lindhardt, A. T.; Skrydstrup, T. *J. Am. Chem. Soc.* **2015**, *137*, 14043–14046.

(39) Beharry, A. A.; Woolley, G. A. *Chem. Soc. Rev.* **2011**, *40*, 4422.

(40) *Molecular Switches*; Feringa, B. L., Browne, W. R., Eds.; Wiley-VCH Verlag GmbH & Co. KGaA: Weinheim, Germany, **2011**.

(41) Holden, M. T. G.; Ram Chhabra, S.; De Nys, R.; Stead, P.; Bainton, N. J.; Hill, P. J.; Manefield, M.; Kumar, N.; Labatte, M.; England, D.; Rice, S.; Givskov, M.; Salmond, G. P. C.; Stewart, G. S. A. B.; Bycrofft B. W., Kjelleberg, S.; Williams P. *Mol. Microbiol.* **2002**, *33*, 1254–1266.

(42) Winson, M. K.; Swift, S.; Fish, L.; Throup, J. P.; Jorgensen, F.; Chhabra, S. R.; Bycroft, B. W.; Williams, P.; Stewart, G. S. A. *FEMS Microbiol. Lett.* **1998**, *163*, 185–192.

(43) Morkunas, B.; Galloway, W. R. J. D.; Wright, M.; Ibbeson, B. M.; Hodgkinson, J. T.; O'Connell, K. M. G.; Bartolucci, N.; Valle, M. Della; Welch, M.; Spring, D. R. *Org. Biomol. Chem.* **2012**, *10*, 8452.

(44) Mattmann, M. E.; Geske, G. D.; Worzalla, G. A.; Chandler, J. R.; Sappington, K. J.; Greenberg, E. P.; Blackwell, H. E. *Bioorg. Med. Chem. Lett.* **2008**, *18*, 3072–3075.

(45) Knoll, J. D.; Turro, C. *Coord. Chem. Rev.* **2015**, *282–283*, 110–126.